

## Replica symmetry breaking in random lasers: A Monte Carlo study with mean-field interacting photonic random walkers

Guillermo Palacios <sup>1,\*</sup>, André C. A. Siqueira <sup>2</sup>, Cid B. de Araújo <sup>2</sup>, Anderson S. L. Gomes <sup>2</sup>, and Ernesto P. Raposo <sup>3</sup>

<sup>1</sup>*Comissão Nacional de Energia Nuclear, Centro Regional de Ciências Nucleares do Nordeste, 50740-545 Recife, Pernambuco, Brazil*

<sup>2</sup>*Departamento de Física, Universidade Federal de Pernambuco, 50670-901 Recife, Pernambuco, Brazil*

<sup>3</sup>*Laboratório de Física Teórica e Computacional, Departamento de Física, Universidade Federal de Pernambuco, 50670-901 Recife, Pernambuco, Brazil*



(Received 21 April 2023; accepted 5 June 2023; published 16 June 2023)

We investigate the replica symmetry breaking (RSB) phenomenon in random lasers (RLs) through Monte Carlo simulations employing photonic random walkers that diffuse and get randomly scattered in the active medium. The walkers interact not only with the population of excited atoms, but also among themselves, in a mean-field-type approach based on the Langevin equation for the stochastic dynamics of RL modes. We obtain the proper profile of the distribution  $P(q)$  of the Parisi overlap parameter in the RSB glassy phase, with two pronounced side maxima at  $q = \pm 1$  above the RL threshold, in contrast with some recent numerical studies. Remarkably, when the interactions among photonic walkers are not included, a replica-symmetric profile with a single maximum of  $P(q)$  at  $q = 0$  is found for any excitation energy. We further study the Gaussian and Lévy emission regimes and statistical correlations of intensity fluctuations in distinct modes of the same spectrum, using a Pearson correlation coefficient recently applied to RLs. Our findings are consistent with experimental results for the intensity statistics and  $P(q)$  distributions in RL materials.

DOI: [10.1103/PhysRevA.107.063510](https://doi.org/10.1103/PhysRevA.107.063510)

### I. INTRODUCTION

Random lasers (RLs) [1–11] are nonlinear multimode photonic systems with low-coherence light emission and spectral properties characterized by the presence of fluctuating spikes at the lasing frequencies. The optical feedback responsible for the RL action typically arises from randomly distributed scattering particles or random variations of the refractive index of the active medium with some sort of spatial inhomogeneity. In this sense, the mechanisms underlying the RL behavior notably contrast with those related to the role of the mirrors and gain medium in a usual Fabry-Pérot cavity in conventional lasers.

Since the first unambiguous demonstration of effective RL emission using a colloidal dye plus TiO<sub>2</sub> nanoscatterers [12], a wide diversity of materials have been reported to display RL features, including dyes dissolved in transparent liquids, gels, or liquid crystals with suspended micro- or nanoparticles as light scatterers [13–18], random fiber lasers with rutile [19] or rare-earth [20] particles, powders of semiconductor quantum dots [21,22], and even atomic vapors that present interesting analogies with astrophysical lasers [23]. The increasing interest in RLs comes from both the ongoing perspective of practical applications and the significant theoretical challenges to explain their unique properties. Indeed, on the one hand, applications of RLs are already a reality in diverse areas, e.g., sensing [24], optofluidics [25,26], and imaging [27], and they continue as well to inspire new exciting ideas [28–33]. On the other hand, RLs have been employed as photonic

platforms to advance the understanding of a number of complex systems behaviors, including Lévy statistics and extreme value events [34–52], turbulence [53–55], and the replica symmetry breaking (RSB) phenomenon [56–73]. In particular, the use of RLs as actual systems to probe theoretical predictions from Parisi’s RSB analysis [74–77] of disordered complex systems (such as magnetic spin glasses) can be regarded as an outstanding scientific achievement [78,79].

The concept of RSB was introduced in Parisi’s approach to spin-glass systems in the late 1970s [74–77]. Spin glasses are magnetic systems with some type of intrinsic disorder, e.g., random distribution of spin interactions. Below some critical temperature, spin-glass systems undergo a phase transition to states in which spins “freeze” along random directions, with nontrivial correlations and rather slow dynamics. The system’s free-energy landscape breaks into a large number of local minima that can trap a spin configuration for sufficiently long times to hamper ergodicity and yield metastability and irreversibility effects. Thus, identical systems, with the same distribution of spin interactions and initially prepared under the same conditions (so-called replicas of the spin system), can eventually reach quite distinct states after some thermodynamic evolution, leading to different measures of observables and spin correlation patterns very distinct from those associated with magnetic phases exhibiting conventional long-range orderings [74–77]. In this regime, the system replicas can no longer be considered as physically equivalent (or symmetric) and an RSB scenario emerges in the spin-glass phase.

In the past two decades, the photonics research group of Università di Roma “Sapienza” has remarkably extended [56–65] the concept of RSB to nonlinear multimode optical systems with some sort of inherent disorder. A rich phase

\*Corresponding author: palaciosg226@gmail.com

diagram has been theoretically proposed [56–63] as a function of the input excitation energy and disorder strength, with the photonic counterpart of the magnetic spin-glass phase corresponding to the RSB glassy behavior in RL systems. On the experimental side, the RSB phenomenon had its first demonstration in the glassy phase of a two-dimensional amorphous solid-state RL material [64]. Subsequently, the RSB behavior was reported as well in diverse photonic systems [65–73].

Random laser systems have been investigated also through numerical methods [35–40,43–46,80–91], some of them generically termed Monte Carlo (MC) simulations, albeit with different implementations of stochastic processes. For instance, in a pioneering MC study of the emission properties of RLs [80], performed about one decade before the theoretical proposal [58] of the photonic RSB phase, photons in an active random medium are treated as diffusing random walkers, with probabilities of stimulating emission or being absorbed set from the rate equations for the levels occupation. Rate equations have been approached also using finite-difference time-domain and transfer-matrix techniques in numerical studies of the interplay of localization and amplification in RLs [81,82]. Transfer-matrix [40,83] and MC [84] methods have been applied as well in the weakly scattering regime of RLs, addressing the effect of local pumping and statistics of RL modes and amplified spontaneous-emission spikes.

In [85–87] MC simulations were performed with the photon paths as random walks in a disordered amplifying medium including stimulated-emission and -absorption processes, with cross-section dependence on the wavelength based on Mie theory. By continuously updating the local occupancy of the ground and excited states of the active atoms, investigations were carried out [85–87] on the chaotic behavior, amplified extended modes, and further spectral features of RLs, such as intensity enhancement and bichromaticity. As the excitation energy increases, the Gaussian-to-Lévy statistical crossovers of the probability distribution of emitted intensities also have been studied [43–46] in this approach, as well as the first-passage length of photons as a function of the disorder strength and extreme value events in the RL spectrum. A variant of this method, but with photons of fixed wavelength, considered specific distributions of turning angles and traversed distances between consecutive random scatterings [35]. A similar statistical analysis of emitted intensities, along with the study of correlations of intensity fluctuations, has been performed in a numerical mean-field approach [88].

The different statistical emission regimes of RL systems have been investigated [36–39] also through MC simulations of multiply scattered random walkers displaying a distribution of wavelengths centered at the transition resonance (see also [89]). In this case, each random walker is assigned a given wavelength and carries a certain amount of energy (photons), which can vary due to spontaneous- and stimulated-emission events along the random scattering path. It is assumed that the walkers interact only with the excited atoms of the gain medium. Thus, the effects of gain saturation and spatiotemporal couplings among different random walkers are included in a self-consistent way, since all walkers are driven by the same population distribution of atoms in the excited state [36–39]. We note in passing that the study of the RSB phenomenon in

RLs could not be performed in this approach since, in addition to the coupling with the gain medium, the presence of nonlinear random interactions between modes is actually essential to yield the RSB glassy phase in RL systems [56–65].

On the other hand, the RSB glassy behavior of RLs has been numerically addressed through a parallel tempering (exchange) MC algorithm [90,91]. The approach is based on the photonic Hamiltonian formulation of RL systems, with randomness and nonlinearity ingredients in the mode interactions [56–65]. A finite-size scaling theory has been developed as well to characterize the behavior of the RL close to the glassy phase transition. The order parameter of this transition is Parisi’s replica overlap parameter  $q$  (discussed below) [56–65,74–77]. In the prelasering regime, with excitation energy below the RL threshold value,  $P(q)$  has a single maximum at  $q = 0$ , indicating that replicas are essentially uncorrelated in a replica-symmetric scenario. In contrast, in the photonic glassy phase above threshold,  $P(q)$  displays two side maxima around the correlated and anticorrelated values  $q = +1$  and  $-1$ , respectively. In this case, replicas are no longer symmetric and the RSB regime sets in.

The exchange MC study confirms [90,91] the predictions of the finite-size scaling theory and identifies the universality class of the RL glassy phase transition as being of mean-field type. Interestingly, however, although the side maxima at  $q \approx \pm 1$  in fact have the onset at the RL threshold, the numerical results for  $P(q)$  show that they are not fully developed in the RSB glassy phase above threshold. Instead, the maximum at  $q = 0$  still prevails even in the RSB regime, where in principle it should be lower than the side maxima.

In this work we investigate numerically properties of multimode RL systems, such as the RSB regime, statistics of emitted intensities, and correlation degree between pairs of modes, through a MC approach based on [36–39]. We find that the proper profile of  $P(q)$  in the RSB glassy phase, with two pronounced side maxima at  $q = \pm 1$ , can actually be obtained by introducing mean-field-type interactions between diffusing random walkers, based on the Langevin equation that drives the stochastic dynamics of the optical modes. We also study the Gaussian and Lévy emission regimes as a function of the excitation energy and the statistical correlations of intensity fluctuations in distinct modes of the same spectrum, through the measure of a proper Pearson correlation coefficient applied to RLs [92–98]. Our findings are consistent with experimental results for the intensity statistics and  $P(q)$  distributions in RL materials.

The article is organized as follows. In Sec. II we review the theoretical background for the Hamiltonian formulation and Langevin dynamics of RL systems and describe the details of the MC simulation. Results are presented and discussed in Sec. III. A summary is given in Sec. IV.

## II. THEORETICAL BACKGROUND AND NUMERICAL SIMULATION

### A. Photonic Hamiltonian formulation and Langevin dynamics

The Hamiltonian formulation of nonlinear multimode photonic systems with a random amplifying medium (including RLs) was developed in a series of seminal works

[56–65], which took as the starting point the system-and-bath Hamiltonian model of quantum nonlinear photonic systems with overlapping modes [99,100]. In the semiclassical context, the creation and annihilation quantum operators of the electromagnetic field are replaced by their complex expected values to yield the effective Hamiltonian function

$$\mathcal{H} = \sum_{\{k_1, k_2\}'} g_{k_1, k_2}^{(2)} a_{k_1} a_{k_2}^* + \sum_{\{k_1, k_2, k_3, k_4\}'} g_{k_1, k_2, k_3, k_4}^{(4)} a_{k_1} a_{k_2}^* a_{k_3} a_{k_4}^*, \quad (1)$$

where  $g_{k_1, k_2}^{(2)}$  and  $g_{k_1, k_2, k_3, k_4}^{(4)}$  denote complex quadratic and quartic couplings, respectively, among overlapping slow-amplitude modes  $\{a_k\}$ , with the latter related to the nonlinear optical  $\chi^{(3)}$  susceptibility (see, e.g., [56,91]). The semiclassical approximation is related to the regime with a high density of photons, which represents the case of interest in the present work and also corresponds to the experimental situation considered, e.g., in [64–73]. We also comment that the interactions between modes in a nonlinear optical system can generally give rise to phenomena such as energy transfer between modes and excitation of new modes due to nonlinear interactions. These interactions can be subtle and possibly lead to complex behaviors in radiation dynamics. The information about how modes are nonlinearly coupled in a material is contained in the high-order susceptibilities (third order in our case). In the strong-cavity limit with small losses [61,101], the diagonal elements of  $g_{k_1, k_2}^{(2)}$  dominate over the off-diagonal ones. Moreover,  $g_{k_1, k_2, k_3, k_4}^{(4)}$  carries the signature of the structural randomness of the active medium in RL systems.

In a nonlinear medium, the electric field can be expanded in leading-order perturbation theory [102] on the basis of complex slow-amplitude modes as

$$\mathbf{E}(\mathbf{r}, t) = \text{Re} \left( \sum_k \mathbf{E}_k(\mathbf{r}) a_k(t) e^{i\omega_k t} \right), \quad (2)$$

in which  $\omega_k$  is the frequency of mode  $k$ , with an analogous expression for the magnetic field. The slow-amplitude modes  $a_k(t) = A_k(t) e^{i\phi_k(t)}$  present the dynamics of the real amplitudes  $A_k$  evolving much slower than that of the phases  $\phi_k$ . Thus, in the so-called slow-amplitude approximation [56,91] the phases can be averaged out, with  $\bar{a}_k(\omega) \approx \delta(\omega - \omega_k)$  upon Fourier transformation and  $\delta$  as the Dirac delta function. This implies that only mode combinations with  $|\omega_{k_1} - \omega_{k_2}| \lesssim \gamma$  and  $|\omega_{k_1} - \omega_{k_2} + \omega_{k_3} - \omega_{k_4}| \lesssim \gamma$  are accounted for in the first and second terms of Eq. (1), respectively, where  $\gamma$  is the typical linewidth of modes. These constraints correspond to the frequency matching conditions [56,91] indicated by the terms  $\{k_1, k_2\}'$  and  $\{k_1, k_2, k_3, k_4\}'$  in the sums of Hamiltonian (1). The slow-amplitude modes thus form a suitable basis to describe lasing modes with narrow linewidth around the lasing frequencies. We also comment that the slow-amplitude approximation results from the temporal dynamics of the emitted signal in a random laser, in which the mode amplitudes vary on a much longer timescale when compared to the phases, a circumstance that favors the consideration of the mode amplitudes as quenched (i.e., random but slowly varying) variables.

The explicit calculation from first principles of the second and quartic couplings in Eq. (1) is virtually unfeasible. Thus, for practical purposes one possibility is to assume that their values are taken from some probability density function. For instance, in the statistical physics analysis of multimode photonic systems with a random amplifying medium (e.g., RLs) [56–65], a mean-field-type approach considered the couplings in Eq. (1) as being statistically independent and quenched (i.e., static), with all  $g$ 's of a given (second or fourth) order drawn from the same Gaussian distribution, along with the relaxation of the frequency matching constraints, so that any given combination of modes is allowed. In the slow-amplitude approximation, the energy associated with mode  $k$  in the RL is  $E_k = |a_k|^2 = A_k^2$  (apart from an unimportant proportionality constant). In this sense, the mean-field statistical physics approach to the Hamiltonian (1) also assumed the system in equilibrium with the energy pumping source, leading to the spherical constraint of constant total energy  $E = \sum_k E_k$  in the RL medium.

The stochastic dynamics of the modes is described by the Langevin equation [56,57]

$$\frac{da_k}{dt} = -\frac{\partial \mathcal{H}}{\partial a_k^*} + \xi_k(t), \quad (3)$$

where  $\xi_k(t)$  is an uncorrelated complex white noise in a suitable choice of basis of slow-amplitude modes, which is remnant of the correlated complex quantum noise in [99,100]. The Langevin dynamics of the energies  $E_k$  can be determined also in the strong-cavity limit with frequency matching conditions comprising the modes combinations [59,103]  $\omega_{k_1} = \omega_{k_2}$  and  $\omega_{k_3} = \omega_{k_4}$ ,  $\omega_{k_1} = \omega_{k_4}$  and  $\omega_{k_2} = \omega_{k_3}$ , and  $\omega_{k_1} - \omega_{k_2} = \omega_{k_4} - \omega_{k_3}$ . By usually disregarding the latter and considering  $\text{Re}(g_{kk}^{(2)}) = \alpha_k - \gamma_k$ , with  $\gamma_k$  and  $\alpha_k$  as the amplification (gain) and radiation loss coefficient rates [47,59,101,103], respectively, we find

$$\frac{dE_{k_1}}{dt} = E_{k_1} \left( 2(\gamma_{k_1} - \alpha_{k_1}) - 4\mu E - 4\sigma \sum_{k_3} G_{k_1, k_3} E_{k_3} \right). \quad (4)$$

Above, the quartic couplings are assumed to be Gaussian distributed with mean  $\mu$  and variance  $\sigma^2$ , so they can be generally expressed in the form  $\text{Re}(g_{k_1, k_1, k_3, k_3}^{(4)}) = \text{Re}(g_{k_1, k_3, k_3, k_1}^{(4)}) = \mu + \sigma G_{k_1, k_3}$ , with the values of the quenched random variables  $G_{k_1, k_3}$  taken from a Gaussian with null mean and unit variance. The  $G$  terms with  $k_1 = k_3$  and  $k_1 \neq k_3$  account for the random self- and cross-saturation effects, respectively. We also consider, as in [56–65], that the mean value of the mode couplings is proportional to the square of the excitation energy  $E_t$ , i.e.,  $\mu = \mu_0 E_t^2$ , while the degree of disorder of the RL medium increases with  $\sigma$ . We further notice in the case of additive noise that the noise term is averaged out to zero in the slow-amplitude approximation. The mean-field-type approximation of the coupling between modes in Eq. (4) can be justified from the fact that, differently from spin Hamiltonian models in magnetic systems, each mode in a random laser system is essentially coupled with every other mode due to the spatial overlap.

### B. Monte Carlo simulation

The theoretical formulation above helps shed light on MC algorithms aiming to describe the photonic processes underlying the multiply scattered diffusion of photons in the random amplifying medium of multimode RLs. Concisely (see below for details), we take as the starting point the MC study [36–39] in which photons of a given wavelength are carried by a random walker propagating in a two-dimensional lattice. As many walkers diffuse and eventually get randomly scattered, their number of photons can increase or decrease at each discrete time step, due to either spontaneous emission or stimulated emission (through the interaction with the local population of excited atoms) or upon leaving the lattice. Here, in order to investigate the RSB glassy phase above the RL threshold, we further introduce interactions among the photonic random walkers in a way similar to Eq. (4), discussed below.

The MC simulation was implemented on a square lattice of  $L \times L$  sites at positions  $(x, y)$ , where  $x = 1, 2, \dots, L$  and  $y = 1, 2, \dots, L$  (in lattice spacing units). Initially, the population distribution of excited atoms at time  $t = 0$  is assumed to have a Gaussian spatial shape

$$N(x, y, t = 0) = N_0 \exp\left(-\frac{(x - L/2)^2 + (y - L/2)^2}{2\Sigma^2}\right). \quad (5)$$

Without loss of generality,  $N$  can be considered a continuous variable, with  $N_0$  a constant. Indeed, since random laser systems generally present a large number of elements (e.g., rare-earth ions) responsible for the electronic transitions giving rise to stimulated emissions, a Gaussian distribution of discrete  $N$  values with  $\Delta N/N \ll 1$  approaches a Gaussian distribution of continuous  $N$  values in Eq. (5). As active atoms are excited by an external pumping source, the initial sum of  $N$  over the whole lattice (i.e., the total number of excited atoms at  $t = 0$ ) is proportional to the excitation energy  $E_t$ . In fact, in the numerical procedure we actually set  $E_t$  (in energy units) so that  $N_0 = E_t / \sum_{x,y} N(x, y, t = 0)$ . From Eq. (5) we also note that the input energy is concentrated around the center of the lattice, with dispersion  $\Sigma$  (here we use  $\Sigma = 40$  and  $L = 150$ , yielding  $\Sigma/L \approx 1/4$ ). As described below, the number  $N(x, y, t)$  of excited atoms at position  $(x, y)$  at time  $t$  is a dynamical quantity, which is progressively updated at each time step.

No photonic random walkers exist at  $t = 0$ . In fact, as the time progresses in discrete  $\Delta t = 1$  steps (i.e.,  $t = 1, 2, \dots$  in time units), walkers are continuously created, initially with a single photon due to spontaneous emission taking place at an excited atom. In addition, the random walkers eventually increase their number of carried photons by stimulated emission.

The processes associated with spontaneous and stimulated emissions of photons and random scattering and diffusion of photonic random walkers are considered in our MC simulation in a dynamical recursive way as described in the following.

First, regarding the spontaneous emission, at each time step  $t$  we consider that excited atoms at sites  $(x, y)$  have a probability (per unit time) of emitting a photon due to spontaneous emission given by the product of their local population

$N(x, y, t)$  at the current time and the spontaneous-emission rate  $\gamma_0$  (we set  $\gamma_0 = 10^{-4}$  in inverse time units). If a photon is spontaneously emitted from an excited atom at position  $(x, y)$  at time  $t$ , then we update  $N(x, y, t + \Delta t) = N(x, y, t) - 1$ , with  $\Delta t = 1$ . Moreover, the frequency of this photon is drawn from a Cauchy-Lorentz probability density  $P(\omega)$  with average absolute deviation (width)  $\bar{\omega}$  and centered at the transition resonance frequency  $\omega_0$  [104],

$$P(\omega) = \frac{\bar{\omega}}{\pi[\bar{\omega}^2 + (\omega - \omega_0)^2]}. \quad (6)$$

In fact, here we consider  $N_\omega = 1001$  discrete frequencies  $\omega_k$  (channels of frequency) around  $\omega_0$ , i.e.,  $\omega_k = \omega_0 + k\Delta\omega$  (in frequency units), with  $k = -(N_\omega - 1)/2, \dots, 0, \dots, (N_\omega - 1)/2$ ,  $\Delta\omega = 1$ , and  $\omega_0 = 0$ , without loss of generality, whose relative probabilities are given by Eq. (6) with  $\bar{\omega} = 50$ . The denotation  $n_{i,k_i}(t)$  indicates that the walker  $i$  at position  $(x_i, y_i)$  in time  $t$  carries  $n_{i,k_i}$  photons of frequency  $\omega_{k_i}$ . So the corresponding update of the walker  $i$  that gets one more photon due to spontaneous emission reads  $n_{i,k_i}(t + \Delta t) = n_{i,k_i}(t) + 1$ .

Concerning the diffusion of the photonic random walkers, at each time step every walker moves one lattice spacing to one of the four neighboring sites in the square lattice. Each walker has probability  $p_s$  of changing direction (i.e., getting randomly scattered) to one of the three neighbors that are not ahead (we choose below  $p_s = 0.1$ ). Otherwise, it moves forward to the next site without changing direction, with probability  $1 - p_s$ . We also note that  $p_s$  is inversely related to the mean free path of photons between consecutive random scattering events in the RL medium.

As the random walkers diffuse, at each time step their number of photons (or carried energy) can also vary due to stimulated emission. The energy  $E_k(t)$  associated with mode  $k$  in time  $t$  is given by the sum of the numbers of photons of frequency  $\omega_k$  carried by the walkers,  $E_k(t) = \sum_i \delta_{\omega_k, \omega_{k_i}} n_{i,k_i}(t)$ , up to a proportionality constant, with  $\delta$  the Kronecker delta. Likewise, the total energy in the RL is  $E(t) = \sum_k E_k(t) = \sum_i n_{i,k_i}(t)$ . So, by considering that the walkers interact in a way similar to Eq. (4), we write in the discrete time step procedure

$$\begin{aligned} & \frac{1}{\Delta t} [n_{i,k_i}(t + \Delta t) - n_{i,k_i}(t)] \\ &= n_{i,k_i}(t) \left( \gamma(\omega_{k_i}) N(x_i, y_i, t) - 4\mu E - 4\sigma \sum_{k_j} G_{k_i, k_j} E_{k_j} \right). \end{aligned} \quad (7)$$

As for  $N$ , above we treat  $n_{i,k_i}$  as continuous variables. The first term on the right-hand side of Eq. (7) accounts for the contribution to  $n_{i,k_i}(t + \Delta t)$  from the stimulated-emission process occurring when the walker  $i$  at position  $(x_i, y_i)$  at time  $t$  interacts with the population distribution  $N(x_i, y_i, t)$  of excited atoms in the RL medium. The frequency-dependent stimulated-emission rate is given by [104]

$$\gamma(\omega_k) = \frac{\gamma_0}{1 + (\omega_k/\bar{\omega})^2}. \quad (8)$$

Further, the  $G$  terms in Eq. (7) represent mean-field-type quenched random couplings between walkers, favoring either

the increase or decrease of  $n_{i,k_i}(t + \Delta t)$ , with the values of all  $G_{k_i,k_j}$ 's drawn from the same Gaussian distribution. We note that when the walkers interact only with the excited atoms in the RL medium, i.e., for  $\mu = \sigma = 0$  in Eq. (7), we recover the results of [36–39] (discussed in the next section). Here we focus on the investigation of the system of interacting random walkers for values of  $E_t^2 = \mu/\mu_0$  below, near, and above the RL threshold, with fixed  $\sigma = 1.5 \times 10^{-6}$ . The stimulated-emission process also affects the local population of atoms in the excited state, which is accordingly updated by

$$\begin{aligned} & \frac{1}{\Delta t} [N(x_i, y_i, t + \Delta t) - N(x_i, y_i, t)] \\ & = -n_{i,k_i}(t) \gamma(\omega_{k_i}) N(x_i, y_i, t). \end{aligned} \quad (9)$$

Eventually, a diffusing walker reaches one of the system boundaries ( $x = 1$ ,  $x = L$ ,  $y = 1$ , or  $y = L$ ) and leaves the lattice. In this case, the walker is removed from the simulation and its energy is added to the spectrum of emitted intensities at the corresponding frequency.

One typical simulation run starts at  $t = 0$  and ends at the final time  $t = t_f$ , when the intensity spectrum is recorded. Next we run all over again from  $t = 0$  to  $t = t_f$ , with the same parameters and initial conditions as before and independently drawing the random numbers  $G_{k_i,k_j}$  associated with the nonlinear couplings between modes from the same Gaussian distribution. This procedure defines a replica of the system, with the intensity spectrum denoted by  $I_\gamma(\omega_k)$ , where  $\gamma$  ( $=1, 2, \dots, N_r$ ) is the replica label and  $N_r$  is the number of replicas. Here we use  $t_f = 3000$  and  $N_r = 4800$ .

In order to investigate the RSB regime in the photonic glassy phase of a RL system, we calculate Parisi's correlation parameter of intensity fluctuation overlaps between distinct replicas  $\gamma$  and  $\beta$  [56,57],

$$q_{\gamma\beta} = \frac{\sum_k \Delta I_\gamma(\omega_k) \Delta I_\beta(\omega_k)}{\sqrt{\sum_k [\Delta I_\gamma(\omega_k)]^2} \sqrt{\sum_k [\Delta I_\beta(\omega_k)]^2}}, \quad (10)$$

where  $\Delta I_\gamma(\omega_k) = I_\gamma(\omega_k) - \langle I_\gamma(\omega_k) \rangle$  represents the intensity fluctuation of replica  $\gamma$  at frequency  $\omega_k$  with respect to the replica average intensity  $\langle I_\gamma(\omega_k) \rangle = \sum_\gamma I_\gamma(\omega_k)/N_r$ . By considering all pairs of distinct replicas  $\gamma$  and  $\beta$ , we build the distribution  $P(q)$  of  $q_{\gamma\beta}$  values. As mentioned, a single maximum of  $P(q)$  at  $q = 0$  or two side maxima near  $q = \pm 1$  are indicative of the replica-symmetric or RSB regimes, respectively.

We can also measure the correlation between intensity fluctuations at distinct frequencies in the *same* spectrum, by calculating the Pearson correlation coefficient

$$C_{k_i,k_j} = \frac{\sum_\gamma \Delta I_\gamma(\omega_{k_i}) \Delta I_\gamma(\omega_{k_j})}{\sqrt{\sum_\gamma [\Delta I_\gamma(\omega_{k_i})]^2} \sqrt{\sum_\gamma [\Delta I_\gamma(\omega_{k_j})]^2}}. \quad (11)$$

We notice above that, differently from Parisi's overlap parameter (10), in which the sums in  $k$  consider the same frequency  $\omega_k$  in different replica spectra  $\gamma$  and  $\beta$ , in the coefficient  $C_{k_i,k_j}$  summations in  $\gamma$  relate distinct frequencies  $\omega_{k_i}$  and  $\omega_{k_j}$  in a given replica  $\gamma$ . This Pearson coefficient has been applied [92–98] to study modes correlations in a number of RL systems. A negligible value of  $C_{k_i,k_j}$  implies that fluctuations at distinct frequencies behave nearly uncorrelated, in an average over spectra. On the other hand, a positive (negative)  $C_{k_i,k_j}$

indicates that fluctuations at a given frequency are related to fluctuations with the same (different) sign at a distinct frequency.

Finally, to characterize the statistical emission regimes of the RL, we analyze the distribution  $P(I)$  of emitted intensities for excitation energies  $E_t$  below, near, and above the RL threshold. First, we notice from the output spectra that the largest emitted intensities usually correspond to frequencies within a small interval of width  $\delta\omega$  around the transition resonance  $\omega_0$ , and so we choose  $\delta\omega/N_\omega = 20/1001 \approx 0.02$  in our analysis. For a given  $E_t$ , we fix a frequency  $\omega_k$  in this interval and build the distribution  $P(I)$  from the series  $\{I_\gamma(\omega_k)\}$  of intensity values of the various ( $N_r = 4800$ ) replicas  $\gamma$  at this frequency. We then compare  $P(I)$  with the family of Lévy  $\alpha$ -stable distributions [105], characterized by a stability parameter  $\alpha \in (0, 2]$  (discussed below). A best-fitting procedure yields the value of  $\alpha$  for this frequency. Next the same is performed for the other frequencies in the interval. At the end, an average  $\alpha$  over these frequencies is obtained for the excitation energy  $E_t$ .

### III. RESULTS AND DISCUSSION

We now present the MC numerical results obtained by following the procedures detailed above. We start by considering the system without interactions between the photonic random walkers. In particular, no RSB glassy phase is found in this case, with a replica-symmetric phase emerging for all excitation energies. Noticeably, however, when the walkers are allowed to interact in the mean-field-type approach described in the preceding section, an RSB scenario clearly stands out above the RL threshold.

#### A. Case without interactions between walkers

By making  $\mu = \sigma = 0$  in Eq. (7), the photonic random walkers interact only with the local population distribution  $N(x, y, t)$  of excited atoms in the active medium. This coupling leads to stimulated-emission events with probability proportional to  $\gamma(\omega_k)N(x, y, t)$ , which increase the number of photons of frequency  $\omega_k$  carried by the diffusing walkers.

Figures 1(a)–1(f) show profiles of the intensity spectra and corresponding distribution  $P(q)$  of Parisi overlap parameter (10) for three values of the excitation energy  $E_t$ . The intensity emitted at frequency  $\omega_k$  is proportional to the number of photons of this frequency that leave the lattice in a simulation run. In Figs. 1(a), 1(c), and 1(e), typical spectra of three replicas are shown in different colors (blue, red, and black).

A significant change of behavior can be noticed in these spectra as the excitation energy increases. For the lowest value  $E_t = 10^5$ , Fig. 1(a) presents weak intensity fluctuations for all replicas. On the other hand, Fig. 1(c) displays for  $E_t = 10^6$  strongly fluctuating spikes at frequencies around the transition resonance  $\omega_0$  that vary from replica to replica. As the excitation energy is enhanced further, the magnitude of fluctuations decreases to an intermediate behavior between the previous ones [see Fig. 1(e) for  $E_t = 7.0 \times 10^6$ ].

The picture depicted in Figs. 1(a), 1(c), and 1(e) corresponds to the Gaussian-to-Lévy crossovers found experimentally and numerically in the statistical emission regimes of

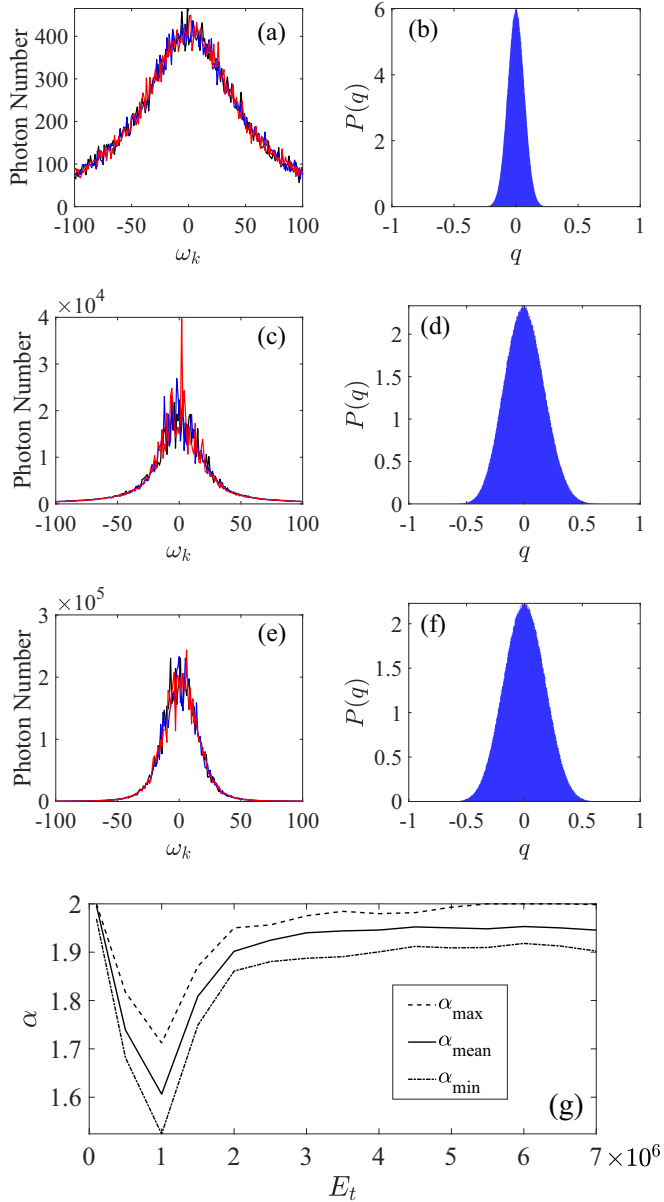


FIG. 1. Case without interactions between photonic random walkers. The intensity spectra and corresponding distribution  $P(q)$  of Parisi overlap parameter values [Eq. (10)] are shown for excitation energies (a) and (b)  $E_t = 10^5$ , (c) and (d)  $E_t = 10^6$ , and (e) and (f)  $E_t = 7.0 \times 10^6$ . The intensity at frequency  $\omega_k$  around the transition resonance set as  $\omega_0 = 0$  is obtained from the number of photons of frequency  $\omega_k$  that leave the lattice in a simulation run. Three typical replica spectra are shown in different colors (blue, red, and black) for each  $E_t$ . The maximum  $P(q)$  at  $q = 0$  signals a replica-symmetric phase, with no RSB for all  $E_t$ . (g) Lévy stability index  $\alpha$  as a function of  $E_t$ . While weak fluctuations are typical of Gaussian behavior [see (a) and (e) with  $\alpha \approx 2$ ], strongly fluctuating intensity spikes emerge in the Lévy regime ( $0 < \alpha < 2$ ), as shown in (c). The solid line in (g) depicts the mean  $\alpha$  over frequencies in a small range of width  $\delta\omega = 20$  centered at  $\omega_0$ , while dash-dotted and dashed lines indicate the minimum and maximum limits of  $\alpha$  from the standard deviation around the average, respectively.

RL systems [34–52]. From a statistical viewpoint, a random variable  $u \in (-\infty, \infty)$  is described by the family of Lévy  $\alpha$ -stable distributions if its probability density function is given by [105]

$$p(u) = \frac{1}{2\pi} \int_{-\infty}^{\infty} dk e^{-|ck|^\alpha [1 - \beta \text{sgn}(k)\Phi(k)] - ik(u-v)}. \quad (12)$$

The Lévy stability index  $\alpha \in (0, 2]$  is the most important parameter since it sets the main statistical properties of  $u$ . Indeed, whereas the borderline value  $\alpha = 2$  leads to the Gaussian distribution, with weak fluctuations in  $u$  governed by the central-limit theorem (CLT), the generalized CLT drives the strong-fluctuation regime for  $0 < \alpha < 2$  [105]. In addition,  $\beta \in [-1, 1]$  is the asymmetry (skewness) parameter,  $c > 0$  is a scale factor,  $v$  is a shift (location) parameter,  $\text{sgn}$  is the sign function,  $\Phi = \tan(\pi\alpha/2)$  if  $\alpha \neq 1$ , and  $\Phi(k) = (-2/\pi) \log |k|$  if  $\alpha = 1$ . Here, with positively defined intensities  $I$ , in practice we consider Lévy distributions  $p(I) = p(|u|) + p(-|u|) = 2p(|u|)$  in the  $I \geq 0$  domain.

Following the procedure described in the preceding section, we obtain intensity distributions  $P(I)$  and fit to Lévy distributions using the quantile-based McCulloch method [106]. In Fig. 1(g) the solid line shows the best-fit value of the Lévy parameter  $\alpha$  averaged over the frequencies in the range of width  $\delta\omega = 20$  centered at the transition resonance  $\omega_0$ . In addition, the dash-dotted and dashed lines depict the minimum and maximum limits of  $\alpha$ , respectively, from the standard deviation around the mean for each  $E_t$ . Consistent with Fig. 1(a), an essentially Gaussian statistical behavior with  $\alpha \approx 2$  is observed in the low- $E_t$  regime. As  $E_t$  is increased, a crossover takes place to a Lévy behavior with  $0 < \alpha < 2$ , which is followed by a trend to return to the Gaussian regime for high  $E_t$ , in agreement with Figs. 1(c) and 1(e).

Despite the presence of intensity spikes typical of the RL regime, the Parisi overlap distribution  $P(q)$  displays a single maximum at  $q = 0$  and the absence of side peaks at  $q = \pm 1$  for all values of  $E_t$ , signaling a replica-symmetric scenario [see Figs. 1(b), 1(d), and 1(f)]. This finding indicates that no RSB glassy regime emerges in the case of noninteracting photonic random walkers, i.e., in the absence of nonlinear random couplings between lasing modes, as expected.

## B. Case with interacting photonic walkers

We next consider photonic walkers with mean-field interactions modulated by the Gaussian random couplings  $G_{k_i, k_j}$  and parameters  $\mu$  and  $\sigma$  in Eq. (7).

Figures 2(a)–2(d) present the distribution  $P(q)$  for a number of excitation energies  $E_t = 10^6$ ,  $5.0 \times 10^6$ ,  $5.5 \times 10^6$ , and  $8.0 \times 10^6$ , respectively. We notice that when the interactions between walkers are turned on, an RSB scenario is clearly evidenced in the RL regime above  $E_t \approx 5.0 \times 10^6$ . In particular, in contrast to Fig. 1,  $P(q)$  displays pronounced side maxima at  $q = \pm 1$  for  $E_t = 8.0 \times 10^6$ , as seen in Fig. 2(d). These results are corroborated by Fig. 2(e), which shows the absolute value  $|q_{\max}|$  at which  $P(q)$  is maximum. A transition from the replica symmetric to the RSB phase is

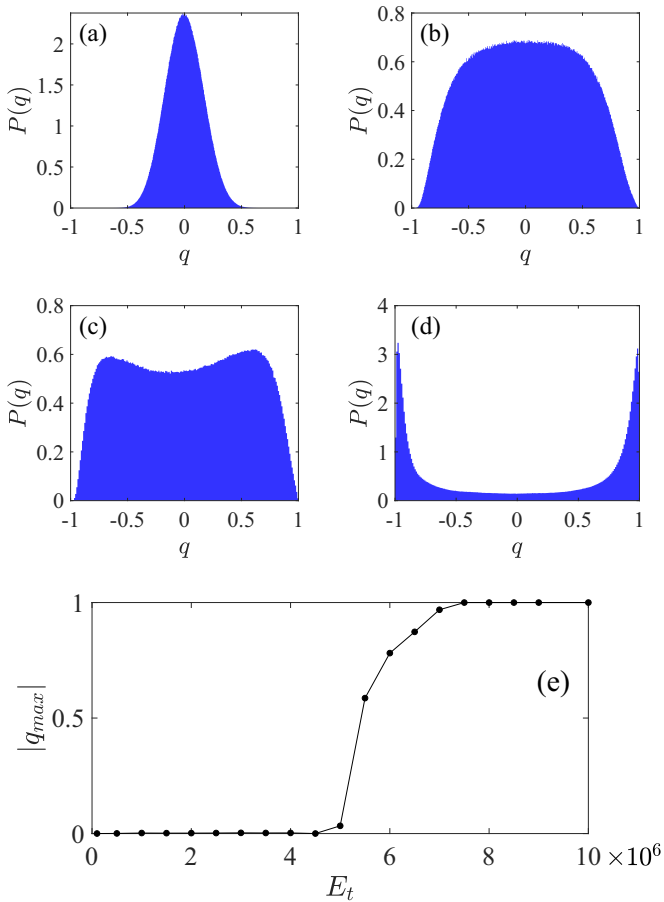


FIG. 2. Case with interactions between photonic random walkers. The distribution  $P(q)$  of Parisi overlap parameter values [Eq. (10)] is shown for excitation energies (a)  $E_t = 10^6$ , (b)  $E_t = 5.0 \times 10^6$ , (c)  $E_t = 5.5 \times 10^6$ , and (d)  $E_t = 8.0 \times 10^6$ . (a) A pronounced maximum in  $P(q)$  at  $q = 0$  signals a prelasing replica-symmetric phase. (b) and (c) As  $E_t$  increases, a slightly bimodal  $P(q)$  with maxima at  $|q| \gtrsim 0$  indicates the onset of an RSB glassy phase at the RL threshold (compare with the replica-symmetric phase for all  $E_t$  in Fig. 1, in the absence of interactions between walkers). (d) For higher  $E_t$  above threshold, the RSB side maxima occur at  $q = \pm 1$ . (e) Absolute value  $|q_{max}|$  at which  $P(q)$  is maximum as a function of  $E_t$ , showing that the transition from the replica symmetric to the RSB phase takes place around  $E_t \approx 5.0 \times 10^6$ .

observed around  $E_t \approx 5.0 \times 10^6$ . We mention that profiles of the distribution  $P(q)$  similar to those shown in Fig. 2 have been experimentally found in RL materials with a transition from prelasing replica-symmetric to RSB glassy phases above threshold [64–73,96,97] (see, for example, Fig. 2 in [66], Figs. 2 and 3 in [96], and Fig. 2 in [97]).

Figure 3 depicts the Lévy parameter  $\alpha$  for two representative frequencies  $\omega_k$  in the small interval of width  $\delta\omega$  around  $\omega_0$ , as a function of  $E_t$ . Both curves display the same qualitative evolution, starting from the Gaussian regime with  $\alpha \approx 2$  for low  $E_t$ , shifting to a Lévy statistical regime with  $0 < \alpha < 2$ , and subsequently tending to return to Gaussian statistics for high  $E_t$ . The quantitative differences in the plots arise from the distinct sets of nonlinear couplings  $\{G_{k_i,k_j}\}$

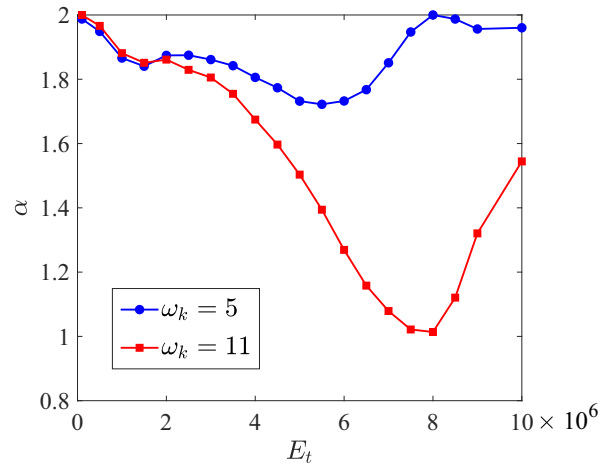


FIG. 3. Lévy parameter  $\alpha$  for two frequencies in the small interval of width  $\delta\omega$  around the transition resonance  $\omega_0$ , as a function of the excitation energy  $E_t$ . As  $E_t$  increases, a regime with Gaussian intensity fluctuations ( $\alpha \approx 2$ ) for low  $E_t$  is followed by a Lévy statistical behavior ( $0 < \alpha < 2$ ) and by a subsequent trend to return to the Gaussian statistics for higher  $E_t$ .

which are stochastically assigned in Eq. (7) to each random walker of frequency  $\omega_{k_i}$  that interacts with all other walkers of frequencies  $\omega_{k_j}$ .

By comparing Figs. 2(e) and 3, we notice that the transition to the RSB phase at  $E_t \approx 5.0 \times 10^6$  does not coincide with the onset of the Lévy statistical regime. In fact, though some of the first reports [49,66] of the RSB phase and Lévy intensity statistics in the same RL suggested a simultaneous emergence of both phenomena, other accounts have noted [65] that their onsets may not match, with the hint that the RL threshold should concur with the transition to the RSB regime.

Finally, we analyze the statistical correlations between intensity fluctuations of pairs of frequencies  $\omega_{k_i}$  and  $\omega_{k_j}$  in the same spectrum, through the Pearson coefficient  $C_{k_i,k_j}$  [Eq. (11)]. It has been experimentally shown [88,95,107] that, by tuning the excitation energy near the RL threshold, it is possible to control the intensity correlations between RL modes from the characterization of the Lévy-like power-law statistics of the emission spectrum survival function. Nevertheless, it is also important to note that in many cases, due to the low resolution of the spectral measurement, this kind of analysis may be difficult and imprecise. In spite of this, interesting applications can arise from the control of the correlations between specific RL modes, such as in biomedical settings and network communications [107].

In the present context, correlations  $C_{k_i,k_j}$  in the intensity fluctuations are shown in Fig. 4(a) for nine chosen pairs of frequencies as a function of  $E_t$ . We first observe, for low  $E_t$ , that all pairs in the same spectrum are essentially uncorrelated, with  $C_{k_i,k_j} \approx 0$ . As  $E_t$  is increased, three distinct behaviors arise: The pairs of modes remain nearly uncorrelated even for high  $E_t$  (black lines) or shift behavior to a correlated (red,  $C_{k_i,k_j} > 0$ ) or anticorrelated (blue,  $C_{k_i,k_j} < 0$ ) regime. A further increase in  $E_t$  tends to saturation of the correlated

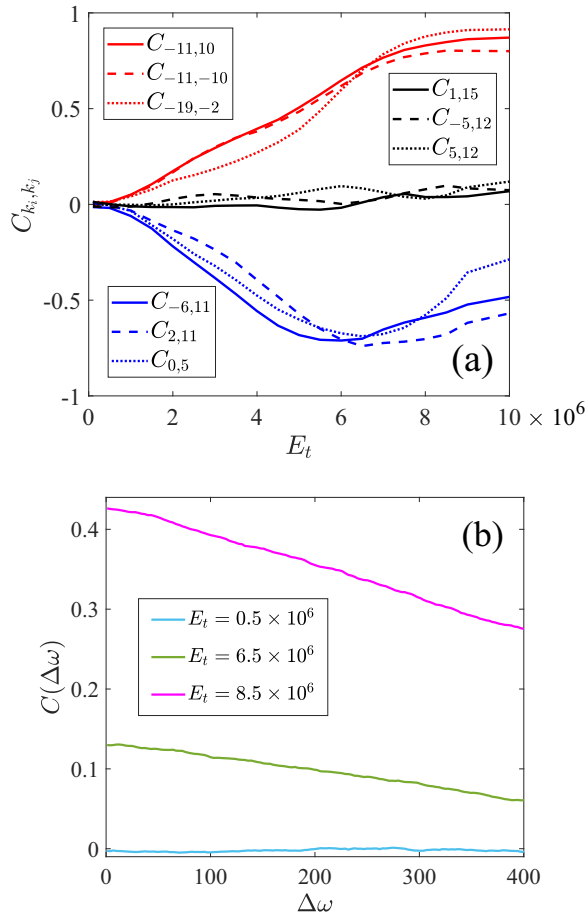


FIG. 4. Pearson correlation coefficient  $C_{k_i, k_j}$  [Eq. (11)] for intensity fluctuations of (a) nine chosen pairs of frequencies  $\omega_{k_i}$  and  $\omega_{k_j}$  in the same spectrum, as a function of the excitation energy  $E_t$ , and (b) frequency separation  $\Delta\omega = |\omega_{k_i} - \omega_{k_j}|$ . (a) The uncorrelated behavior  $C_{k_i, k_j} \approx 0$  observed for all pairs and low  $E_t$  shifts, as  $E_t$  increases, to either correlated ( $C_{k_i, k_j} > 0$ , red) or anticorrelated ( $C_{k_i, k_j} < 0$ , blue) regimes or, in a smaller number of cases, remains with  $C_{k_i, k_j} \approx 0$  (black). (b) More separated frequencies in the same spectrum generally give rise to weaker correlations.

and anticorrelated modes while still keeping unchanged the uncorrelated modes behavior of some pairs.

The results of Fig. 4(a) are complemented by the analysis shown in Fig. 4(b) of the behavior of  $C_{k_i, k_j}$  as a function of the frequency separation  $\Delta\omega = |k_i - k_j|$ . In the low- $E_t$  regime frequencies are uncorrelated no matter how separated they are in the intensity spectrum (black line,  $E_t = 5.0 \times 10^5$ ), as expected. In contrast, we notice a nearly monotonic decrease of  $C_{k_i, k_j}$  with  $\Delta\omega$  for higher  $E_t$ , indicating that modes that

are closer in the same spectrum generally display stronger correlations (see the blue and red lines for  $E_t = 6.5 \times 10^6$  and  $8.5 \times 10^6$ , respectively).

#### IV. CONCLUSION

The importance of advancing the understanding of random laser systems can hardly be overstated. Random lasers have already provided various practical applications [1,2,24–27] and continue as well to inspire new exciting ideas [28–33]. Moreover, in parallel to the theoretical challenges posed to explain their features, RLs also have been employed [1,2] as photonic platforms to study complex systems behaviors, such as unconventional Lévy statistics, turbulence, and the replica symmetry breaking phenomenon.

In this work we have investigated RL systems through Monte Carlo simulations employing photonic random walkers that diffuse and get randomly scattered in the active medium. The walkers interact not only with the population of atoms in the excited state, yielding spontaneous-emission events, but also among themselves, in a mean-field-type approach based on the Langevin equation that drives the stochastic dynamics of RL modes.

In particular, we have obtained the proper profile of the distribution  $P(q)$  of the Parisi overlap parameter in the RSB glassy phase, with two pronounced side maxima at  $q = \pm 1$  above the RL threshold. Noticeably, when the interactions between photonic walkers are not taken into account, a replica-symmetric profile with a single maximum of  $P(q)$  at  $q = 0$  is found for any excitation energy.

We have also concomitantly studied the Gaussian and Lévy statistical emission regimes of the RL system. Our findings are consistent as well with the analysis of the statistical correlations of intensity fluctuations in distinct modes of the same spectrum, through the measure of a suitable Pearson correlation coefficient.

We hope our work can stimulate further experimental, theoretical, and numerical investigations of RLs and, more generally, of photonic systems with some type of inherent randomness.

#### ACKNOWLEDGMENTS

The authors are grateful for financial support from the Brazilian agencies Conselho Nacional de Desenvolvimento Científico e Tecnológico, Fundação de Amparo à Ciência e Tecnologia do Estado de Pernambuco (Núcleo de Excelência em Nanofotônica e Biofotônica–Nanobio and Núcleo de Excelência em Modelagem de Processos e Fenômenos Físicos em Materiais e Sistemas Complexos), and Instituto Nacional de Fotônica (INCT project).

- [1] *Lévy Statistics and Spin Glass Behavior in Random Lasers*, edited by A. S. L. Gomes, A. L. Moura, C. B. de Araújo, and E. P. Raposo (Taylor & Francis, New York, 2023).  
 [2] A. S. L. Gomes, A. L. Moura, C. B. de Araújo, and E. P. Raposo, Recent advances and applications of random lasers

and random fiber lasers, *Prog. Quantum Electron.* **78**, 100343 (2021).

- [3] I. Viola, L. Leuzzi, C. Conti, and N. Ghofraniha, in *Organic Lasers*, edited by M. Anni and S. Lattante (Jenny Stanford Publishing, Singapore, 2018), p. 151.

- [4] D. V. Churkin, S. Sugavanam, I. D. Vatnik, Z. Wang, E. V. Podivilov, S. A. Babin, Y. Rao, and S. K. Turitsyn, Recent advances in fundamentals and applications of random fiber lasers, *Adv. Opt. Photon.* **7**, 516 (2015).
- [5] F. Luan, B. Gu, A. S. L. Gomes, K.-T. Yong, S. Wen, and P. N. Prasad, Lasing in nanocomposite random media, *Nano Today* **10**, 168 (2015).
- [6] L. Miao, S. Tanemura, H. Yang, and S. P. Lau, Synthesis and random laser application of ZnO nano-walls: A review, *Int. J. Nanotechnol.* **6**, 723 (2009).
- [7] D. S. Wiersma, The physics and applications of random lasers, *Nat. Phys.* **4**, 359 (2008).
- [8] H. Cao, Review on latest developments in random lasers with coherent feedback, *J. Phys. A: Math. Gen.* **38**, 10497 (2005).
- [9] M. A. Noginov, *Solid-State Random Lasers* (Springer, Berlin, 2005).
- [10] A. L. Moura, S. J. Carreño, P. I. R. Pincheira, L. J. Q. Maia, V. Jerez, E. P. Raposo, A. S. L. Gomes, and C. B. de Araújo, Non-linear effects and photonic phase transitions in Nd<sup>3+</sup>-doped nanocrystal-based random lasers, *Appl. Opt.* **59**, D155 (2020).
- [11] C. B. de Araújo, A. S. L. Gomes, and E. P. Raposo, Lévy statistics and the glassy behavior of light in random fiber lasers, *Appl. Sci.* **7**, 644 (2017).
- [12] N. M. Lawandy, R. M. Balachandran, A. S. L. Gomes, and E. Sauvain, Laser action in scattering media, *Nature (London)* **368**, 436 (1994).
- [13] L. Ye, C. Zhao, Y. Feng, B. Gu, Y. Cui, and Y. Lu, Study on the polarization of random lasers from dye-doped nematic liquid crystals, *Nanoscale Res. Lett.* **12**, 27 (2017).
- [14] L. M. G. Abegão, D. S. Manoel, A. J. G. Otuka, P. H. D. Ferreira, D. R. Vollet, D. A. Donatti, L. D. Boni, C. R. Mendonça, F. S. D. Vicente, J. J. Rodrigues, and M. A. R. C. Alencar, Random laser emission from a rhodamine B-doped GPTS/TEOS-derived organic/silica monolithic xerogel, *Laser Phys. Lett.* **14**, 065801 (2017).
- [15] M. Shasti, P. Coutino, S. Mukherjee, A. Varanytsia, T. Smith, A. P. Luchette, L. Sukhomlinova, T. Kosa, A. Munoz, and B. Taheri, Reverse mode switching of the random laser emission in dye doped liquid crystals under homogeneous and inhomogeneous electric fields, *Photon. Res.* **4**, 7 (2016).
- [16] B. R. Anderson, R. Gunawidjaja, and H. Eilers, Self-healing organic-dye-based random lasers, *Opt. Lett.* **40**, 577 (2015).
- [17] A. S. L. Gomes, M. T. Carvalho, C. T. Dominguez, C. B. de Araújo, and P. N. Prasad, Direct three-photon excitation of upconversion random laser emission in a weakly scattering organic colloidal system, *Opt. Express* **22**, 14305 (2014).
- [18] S. Knitter, M. Kues, and C. Fallnich, Emission polarization of random lasers in organic dye solutions, *Opt. Lett.* **37**, 3621 (2012).
- [19] C. J. S. de Matos, L. de S. Menezes, A. M. Brito-Silva, M. A. Martínez Gámez, A. S. L. Gomes, and C. B. de Araújo, Random Fiber Laser, *Phys. Rev. Lett.* **99**, 153903 (2007).
- [20] M. Gagné and R. Kashyap, Demonstration of a 3 mW threshold Er-doped random fiber laser based on a unique fiber Bragg grating, *Opt. Express* **17**, 19067 (2009).
- [21] Y. Chen, J. Herrnsdorf, B. Guilhabert, Y. Zhang, I. M. Watson, E. Gu, N. Laurand, and M. D. Dawson, Colloidal quantum dot random laser, *Opt. Express* **19**, 2996 (2011).
- [22] C. T. Dominguez, M. A. Gomes, Z. S. Macedo, C. B. de Araújo, and A. S. L. Gomes, Multi-photon excited coherent random laser emission in ZnO powders, *Nanoscale* **7**, 317 (2015).
- [23] Q. Baudouin, N. Mercadier, V. Guarrera, W. Guerin, and R. Kaiser, A cold-atom random laser, *Nat. Phys.* **9**, 357 (2013).
- [24] E. Ignesti, F. Tommasi, L. Fini, F. Martelli, N. Azzali, and S. Cavalieri, A new class of optical sensors: A random laser based device, *Sci. Rep.* **6**, 35225 (2016).
- [25] B. N. S. Bhaktha, N. Bachelard, X. Noblin, and P. Sebbah, Optofluidic random laser, *Appl. Phys. Lett.* **101**, 151101 (2012).
- [26] N. Bachelard, S. Gigan, X. Noblin, and P. Sebbah, Adaptive pumping for spectral control of random lasers, *Nat. Phys.* **10**, 426 (2014).
- [27] B. Redding, M. A. Choma, and H. Cao, Speckle-free laser imaging using random laser illumination, *Nat. Photon.* **6**, 355 (2012).
- [28] A. Consoli, N. Caselli, and C. López, Electrically driven random lasing from a modified Fabry-Pérot laser diode, *Nat. Photon.* **16**, 219 (2022).
- [29] H. Zhang, J. Wu, Y. Wan, P. Wang, B. Yang, X. Xi, X. Wang, and P. Zhou, Kilowatt random Raman fiber laser with full-open cavity, *Opt. Lett.* **47**, 493 (2022).
- [30] A. Thompson, Random fiber laser could drive next generation fusion experiments, *SciLight* **2023**, 041106 (2023).
- [31] M. Fan, S. Lin, K. Yao, Y. Qi, J. Zhang, J. Zheng, P. Wang, L. Ni, X. Bao, D. Zhou, B. Zhang, K. Xiao, H. Xia, R. Zhang, P. Li, W. Zheng, and Z. Wang, Spectrum-tailored random fiber laser towards ICF laser facility, *Matter Radiat. Extremes* **8**, 025902 (2023).
- [32] S. Li, J. Xu, J. Liang, J. Ye, Y. Zhang, X. Ma, J. Leng, and P. Zhou, Multi-wavelength random fiber laser with a spectral-flexible characteristic, *Photon. Res.* **11**, 159 (2023).
- [33] A. Consoli, N. Caselli, and C. López, Networks of random lasers: Current perspective and future challenges, *Opt. Mater. Express* **13**, 1060 (2023).
- [34] D. Sharma, H. Ramachandran, and N. Kumar, Lévy statistical fluctuations from a random amplifying medium, *Fluct. Noise Lett.* **06**, L95 (2006).
- [35] D. Sharma, H. Ramachandran, and N. Kumar, Gaussian-to-Lévy statistical crossover in a random amplifying medium: Monte Carlo simulation, *Opt. Commun.* **273**, 1 (2007).
- [36] S. Lepri, S. Cavalieri, G.-L. Oppo, and D. S. Wiersma, Statistical regimes of random laser fluctuations, *Phys. Rev. A* **75**, 063820 (2007).
- [37] E. Ignesti, F. Tommasi, L. Fini, S. Lepri, V. Radhalakshmi, D. Wiersma, and S. Cavalieri, Experimental and theoretical investigation of statistical regimes in random laser emission, *Phys. Rev. A* **88**, 033820 (2013).
- [38] F. Tommasi, E. Ignesti, L. Fini, and S. Cavalieri, Controlling directionality and the statistical regime of the random laser emission, *Phys. Rev. A* **91**, 033820 (2015).
- [39] F. Tommasi, L. Fini, E. Ignesti, S. Lepri, F. Martelli, and S. Cavalieri, Statistical outliers in random laser emission, *Phys. Rev. A* **98**, 053816 (2018).
- [40] X. Wu and H. Cao, Statistical studies of random-lasing modes and amplified spontaneous-emission spikes in weakly scattering systems, *Phys. Rev. A* **77**, 013832 (2008).
- [41] R. Uppu and S. Mujumdar, Statistical fluctuations of coherent and incoherent intensity in random lasers with nonresonant feedback, *Opt. Lett.* **35**, 2831 (2010).

- [42] R. Uppu, A. K. Tiwari, and S. Mujumdar, Identification of statistical regimes and crossovers in coherent random laser emission, *Opt. Lett.* **37**, 662 (2012).
- [43] R. Uppu and S. Mujumdar, Dependence of the Gaussian-Lévy transition on the disorder strength in random lasers, *Phys. Rev. A* **87**, 013822 (2013).
- [44] R. Uppu and S. Mujumdar, Lévy exponents as universal identifiers of threshold and criticality in random lasers, *Phys. Rev. A* **90**, 025801 (2014).
- [45] R. Uppu and S. Mujumdar, Exponentially Tempered Lévy Sums in Random Lasers, *Phys. Rev. Lett.* **114**, 183903 (2015).
- [46] R. Uppu and S. Mujumdar, Physical manifestation of extreme events in random lasers, *Opt. Lett.* **40**, 5046 (2015).
- [47] E. P. Raposo and A. S. L. Gomes, Analytical solution for the Lévy-like steady-state distribution of intensities in random lasers, *Phys. Rev. A* **91**, 043827 (2015).
- [48] B. C. Lima, P. I. R. Pincheira, E. P. Raposo, L. de S. Menezes, C. B. de Araújo, A. S. L. Gomes, and R. Kashyap, Extreme-value statistics of intensities in a cw-pumped random fiber laser, *Phys. Rev. A* **96**, 013834 (2017).
- [49] B. C. Lima, A. S. L. Gomes, P. I. R. Pincheira, A. L. Moura, M. Gagné, E. P. Raposo, C. B. de Araújo, and R. Kashyap, Observation of Lévy statistics in one-dimensional erbium-based random fiber laser, *J. Opt. Soc. Am. B* **34**, 293 (2017).
- [50] I. R. R. González, E. P. Raposo, S. J. Carreño, A. M. S. Macêdo, M. Maldonado, L. de S. Menezes, A. S. L. Gomes, and C. B. de Araújo, Influence of fifth-order nonlinearities on the statistical fluctuations in emission intensities in a photonic open-cavity complex system, *Phys. Rev. A* **102**, 063515 (2020).
- [51] I. R. R. González, P. I. R. Pincheira, A. M. S. Macêdo, L. de S. Menezes, A. S. L. Gomes, and E. P. Raposo, Intensity distribution in random lasers: Comparison between a stochastic differential model of interacting modes and random phase sum-based models, *J. Opt. Soc. Am. B* **38**, 2391 (2021).
- [52] J. Li, H. Wu, Z. Wang, S. Lin, C. Lu, E. P. Raposo, A. S. L. Gomes, and Y. Rao, Lévy spectral intensity statistics in a Raman random fiber laser, *Opt. Lett.* **44**, 2799 (2019).
- [53] I. R. R. González, B. C. Lima, P. I. R. Pincheira, A. A. Brum, A. M. S. Macêdo, G. L. Vasconcelos, L. de S. Menezes, E. P. Raposo, A. S. L. Gomes, and R. Kashyap, Turbulence hierarchy in a random fibre laser, *Nat. Commun.* **8**, 15731 (2017).
- [54] I. R. R. González, E. P. Raposo, A. M. S. Macêdo, L. de S. Menezes, and A. S. L. Gomes, Coexistence of turbulence-like and glassy behaviours in a photonic system, *Sci. Rep.* **8**, 17046 (2018).
- [55] A. M. S. Macêdo, I. R. R. González, E. P. Raposo, L. de S. Menezes, and A. S. L. Gomes, Turbulent intermittency in a random fiber laser, *Atoms* **7**, 43 (2019).
- [56] F. Antenucci, *Statistical Physics of Wave Interactions* (Springer, Berlin, 2016).
- [57] F. Antenucci, A. Crisanti, M. Ibáñez-Berganza, A. Marruzzo, and L. Leuzzi, Statistical mechanics models for multimode lasers and random lasers, *Philos. Mag.* **96**, 704 (2016).
- [58] L. Angelani, C. Conti, G. Ruocco, and F. Zamponi, Glassy Behavior of Light, *Phys. Rev. Lett.* **96**, 065702 (2006).
- [59] L. Angelani, C. Conti, G. Ruocco, and F. Zamponi, Glassy behavior of light in random lasers, *Phys. Rev. B* **74**, 104207 (2006).
- [60] L. Leuzzi, C. Conti, V. Folli, L. Angelani, and G. Ruocco, Phase Diagram and Complexity of Mode-Locked Lasers: From Order to Disorder, *Phys. Rev. Lett.* **102**, 083901 (2009).
- [61] F. Antenucci, C. Conti, A. Crisanti, and L. Leuzzi, General Phase Diagram of Multimodal Ordered and Disordered Lasers in Closed and Open Cavities, *Phys. Rev. Lett.* **114**, 043901 (2015).
- [62] F. Antenucci, A. Crisanti, and L. Leuzzi, Complex spherical  $2 + 4$  spin glass: A model for nonlinear optics in random media, *Phys. Rev. A* **91**, 053816 (2015).
- [63] F. Antenucci, A. Crisanti, and L. Leuzzi, The glassy random laser: Replica symmetry breaking in the intensity fluctuations of emission spectra, *Sci. Rep.* **5**, 16792 (2015).
- [64] N. Ghofraniha, I. Viola, F. Di Maria, G. Barbarella, G. Gigli, L. Leuzzi, and C. Conti, Experimental evidence of replica symmetry breaking in random lasers, *Nat. Commun.* **6**, 6058 (2015).
- [65] F. Tommasi, E. Ignesti, S. Lepri, and S. Cavalieri, Robustness of replica symmetry breaking phenomenology in random laser, *Sci. Rep.* **6**, 37113 (2016).
- [66] A. S. L. Gomes, E. P. Raposo, A. L. Moura, S. I. Fewo, P. I. R. Pincheira, V. Jerez, L. J. Q. Maia, and C. B. de Araújo, Observation of Lévy distribution and replica symmetry breaking in random lasers from a single set of measurements, *Sci. Rep.* **6**, 27987 (2016).
- [67] A. S. L. Gomes, B. C. Lima, P. I. R. Pincheira, A. L. Moura, M. Gagné, E. P. Raposo, C. B. de Araújo, and R. Kashyap, Glassy behavior in a one-dimensional continuous-wave erbium-doped random fiber laser, *Phys. Rev. A* **94**, 011801(R) (2016).
- [68] P. I. R. Pincheira, A. F. Silva, S. I. Fewo, S. J. M. Carreño, A. L. Moura, E. P. Raposo, A. S. L. Gomes, and C. B. de Araújo, Observation of photonic paramagnetic to spin-glass transition in a specially designed TiO<sub>2</sub> particle-based dye-colloidal random laser, *Opt. Lett.* **41**, 3459 (2016).
- [69] A. L. Moura, P. I. R. Pincheira, A. S. Reyna, E. P. Raposo, A. S. L. Gomes, and C. B. de Araújo, Replica Symmetry Breaking in the Photonic Ferromagneticlike Spontaneous Mode-Locking Phase of a Multimode Nd:YAG Laser, *Phys. Rev. Lett.* **119**, 163902 (2017).
- [70] S. Basak, A. Blanco, and C. López, Large fluctuations at the lasing threshold of solid- and liquid-state dye lasers, *Sci. Rep.* **6**, 32134 (2016).
- [71] D. Pierangeli, A. Tavani, F. Di Mei, A. J. Agranat, C. Conti, and E. DelRe, Observation of replica symmetry breaking in disordered nonlinear wave propagation, *Nat. Commun.* **8**, 1501 (2017).
- [72] A. Sarkar and B. N. S. Bhaktha, Replica symmetry breaking in coherent and incoherent random lasing modes, *Opt. Lett.* **46**, 5169 (2021).
- [73] Z. Zhou, L. Chen, and X. Bao, High efficiency Brillouin random fiber laser with replica symmetry breaking enabled by random fiber grating, *Opt. Express* **29**, 6532 (2021).
- [74] G. Parisi, Toward a mean field theory for spin glasses, *Phys. Lett. A* **73**, 203 (1979).
- [75] G. Parisi, Infinite Number of Order Parameters for Spin-Glasses, *Phys. Rev. Lett.* **43**, 1754 (1979).
- [76] M. Mézard, G. Parisi, and M. A. Virasoro, *Spin Glass Theory and Beyond* (World Scientific, Singapore, 1987).
- [77] G. Parisi, P. Urbani, and F. Zamponi, *Theory of Simple Glasses* (Cambridge University Press, Cambridge, 2020).

- [78] The Nobel Committee for Physics, Scientific background on the Nobel Prize in Physics 2021, available at [https://www.nobelprize.org/uploads/2021/10/sciback\\_fy\\_en\\_21.pdf](https://www.nobelprize.org/uploads/2021/10/sciback_fy_en_21.pdf).
- [79] G. Parisi, Nobel Lecture: Multiple equilibria [Rev. Mod. Phys. (to be published)], [arXiv:2304.00580](https://arxiv.org/abs/2304.00580).
- [80] G. A. Berger, M. Kempe, and A. Z. Genack, Dynamics of stimulated emission from random media, *Phys. Rev. E* **56**, 6118 (1997).
- [81] X. Jiang and C. M. Soukoulis, Time Dependent Theory for Random Lasers, *Phys. Rev. Lett.* **85**, 70 (2000).
- [82] X. Jiang and C. M. Soukoulis, Localized random lasing modes and a path for observing localization, *Phys. Rev. E* **65**, 025601(R) (2002).
- [83] X. Wu, J. Andreasen, H. Cao, and A. Yamilov, Effect of local pumping on random laser modes in one dimension, *J. Opt. Soc. Am. B* **24**, A26 (2007).
- [84] X. Wu, W. Fang, A. Yamilov, A. A. Chabanov, A. A. Asatryan, L. C. Botten, and H. Cao, Random lasing in weakly scattering systems, *Phys. Rev. A* **74**, 053812 (2006).
- [85] S. Mujumdar, M. Ricci, R. Torre, and D. S. Wiersma, Amplified Extended Modes in Random Lasers, *Phys. Rev. Lett.* **93**, 053903 (2004).
- [86] S. Mujumdar, V. Türck, R. Torre, and D. S. Wiersma, Chaotic behavior of a random laser with static disorder, *Phys. Rev. A* **76**, 033807 (2007).
- [87] R. Torre, S. Mujumdar, H. Ramachandran, and D. S. Wiersma, Monte Carlo calculations of spectral features in random lasing, *J. Nanophoton.* **4**, 041550 (2010).
- [88] J. W. Merrill, H. Cao, and E. R. Dufresne, Fluctuations and correlations of emission from random lasers, *Phys. Rev. A* **93**, 021801(R) (2016).
- [89] E. G. Rocha, E. P. Santos, B. J. dos Santos, S. S. de Albuquerque, P. I. R. Pincheira, C. Argolo, and A. L. Moura, Lévy flights for light in ordered lasers, *Phys. Rev. A* **101**, 023820 (2020).
- [90] G. Gradenigo, F. antenucci, and L. Leuzzi, Glassiness and lack of equipartition in random lasers: The common roots of ergodicity breaking in disordered and nonlinear systems, *Phys. Rev. Res.* **2**, 023399 (2020).
- [91] J. Niedda, G. Gradenigo, L. Leuzzi, and G. Parisi, Universality class of the glassy random laser, *SciPost Phys.* **14**, 144 (2023).
- [92] M. Montinaro, V. Resta, A. Camposeo, M. Moffa, G. Morello, L. Persano, K. Kazlauskas, S. Jursenas, A. Tomkeviciene, J. V. Grazulevicius, and D. Pisignano, Diverse regimes of mode intensity correlation in nanofiber random lasers through nanoparticle doping, *ACS Photon.* **5**, 1026 (2018).
- [93] M. Leonetti, C. Conti, and C. Lopez, The mode-locking transition of random lasers, *Nat. Photon.* **5**, 615 (2011).
- [94] L. F. Sciuti, L. A. Mercante, D. S. Correa, and L. De Boni, Random laser in dye-doped electrospun nanofibers: Study of laser mode dynamics via temporal mapping of emission spectra using Pearson's correlation, *J. Lumin.* **224**, 117281 (2020).
- [95] A. Sarkar, B. N. S. Bhaktha, and J. Andreasen, Replica symmetry breaking in a weakly scattering optofluidic random laser, *Sci. Rep.* **10**, 2628 (2020).
- [96] E. Coronel, A. Das, I. R. R. González, A. S. L. Gomes, W. Margulis, J. P. von der Weid, and E. P. Raposo, Evaluation of Pearson correlation coefficient and Parisi parameter of replica symmetry breaking in a hybrid electronically addressable random fiber laser, *Opt. Express* **29**, 24422 (2021).
- [97] E. D. Coronel, M. L. da Silva-Neto, A. L. Moura, I. R. R. González, R. S. Pugina, E. G. Hilário, E. G. da Rocha, J. M. A. Caiut, A. S. L. Gomes, and E. P. Raposo, Simultaneous evaluation of intermittency effects, replica symmetry breaking and modes dynamics correlations in a Nd:YAG random laser, *Sci. Rep.* **12**, 1051 (2022).
- [98] E. D. Coronel, A. Das, M. L. da Silva-Neto, I. R. R. González, A. S. L. Gomes, and E. P. Raposo, Statistical analysis of intensity fluctuations in the second harmonic of a multimode Nd:YAG laser through a modified Pearson correlation coefficient, *Phys. Rev. A* **106**, 063515 (2022).
- [99] G. Hackenbroich, C. Viviescas, and F. Haake, Field Quantization for Chaotic Resonators with Overlapping Modes, *Phys. Rev. Lett.* **89**, 083902 (2002).
- [100] C. Viviescas and G. Hackenbroich, Field quantization for open optical cavities, *Phys. Rev. A* **67**, 013805 (2003).
- [101] L. I. Deych, Effects of Spatial Nonuniformity on Laser Dynamics, *Phys. Rev. Lett.* **95**, 043902 (2005).
- [102] H. Nayfeh, *Introduction to Perturbation Techniques* (Wiley, New York, 1993).
- [103] C. L. O'Bryan and M. Sargent, Theory of multimode laser operation, *Phys. Rev. A* **8**, 3071 (1973).
- [104] O. Svelto, *Principles of Lasers* (Springer, Berlin, 2010).
- [105] G. Samorodnitsky and M. S. Taqqu, *Stable Non-Gaussian Random Processes* (Chapman and Hall, New York, 1994).
- [106] J. H. McCulloch, Simple consistent estimators of stable distribution parameters, *Commun. Stat.* **15**, 1109 (1986).
- [107] Y. Zhi, A. Lininger, and G. Strangi, Manipulating random lasing correlations in doped liquid crystals, [arXiv:2208.12421](https://arxiv.org/abs/2208.12421).